

# Compact and light-weight design of a Martin Puplett interferometer for synchrotron radiation beam measurements

Daniel Rossetti, Hubert Baechli, Emanuele Japichino, Urs Ellenberger, Volker Schlott  
Paul Scherrer Institut, 5232 Villigen PSI, Switzerland

## Abstract

*We report on a compact and light-weight design of a Martin Puplett Interferometer (MPI). The instrument is mobile and yet precise enough to characterize synchrotron radiation beam quality. It will replace an existing laboratory setup on the Femto beamline of the Swiss synchrotron light source (SLS). Later on the interferometer will be built in a small series to be used along the planned 250 MeV linear accelerator which will serve as a test section for the planned XFEL project at PSI. The components of the MPI are built in-house except for polarizer gratings and linear translation stages which are commercially available off the shelf. Special attention has been given to use unified design approaches for the various components of the MPI. The mounts, the base-plate and the vacuum chamber of the MPI have high stability which has been verified using ANSYS simulations.*

## 1. Introduction

A Martin Puplett interferometer produces an intensity pattern on a detector plane which is the Fourier transform of the radiation source. Like in a Michelson interferometer the wave packet of pulsed radiation source is splitted into two legs of fixed and of variable length by scanning a moveable mirror over some distance. The recombination of the two displaced wave packets gives an autocorrelation measurement of its size in space. Via Fourier transformation the spectra of the source in the frequency or wavelength domain can be reconstructed. The Martin Puplett interferometer (MPI) uses the state of polarization to split a wave packet instead of using its amplitude as for a Michelson interferometer [1]. Polarizer gratings of MPI have very broadband frequency characteristics and have negligible losses which make them advantageous over coated beam splitters used in Michelson interferometers.

## 2. Existing THz diagnostic setup for bunch slicing project at the Femto beamline of SLS

Sub-picosecond X-ray pulses are generated in the storage ring of the Swiss Light Source (SLS) by resonant interaction of the electron bunches with a sub-picosecond laser pulse in the periodic field of a wiggler magnet (modulator). When subsequently passing an undulator (radiator) the energy modulated electrons emit X-rays with the same sub-picosecond time profile as the laser pulse. Energy modulated electrons form a longitudinal density modulation on the length scale of the laser pulse width (i.e. 100 fs X-ray or laser pulses corresponds to 30  $\mu\text{m}$  long electron bunches). An optical transfer line for visible and long wavelength (THz) synchrotron radiation has been installed after the modulator to allow for longitudinal slicing diagnostics in the Femto beamline experimental area. A MPI using off-the shelf components has been setup on an optical table to measure electron and laser beam overlap and to reconstruct X-ray fs-pulse spectra from measured interferograms as a function of the number of roundtrips after the slicing event [2].

From the experience with the current experimental setup a number of improvements were identified:

- Portable but stable to measure X-ray beam characteristics in the THz-range at other beam locations
- Setup under vacuum ( $< 10^{-2}$  bar) to prevent water absorption lines and to be flanged directly on an existing optical transfer line (better known transfer function with less interfaces)
- Use of large optics ( $> 4 \times$  beam diameter) of diameter of 100 mm to prevent diffraction losses
- Use of wire polarizer gratings (5  $\mu\text{m}$  thick tungsten wire with a spacing of 10  $\mu\text{m}$ ) or of lithographic polarizer gratings (thickness of 1  $\mu\text{m}$  and spacing of 2  $\mu\text{m}$ ) for efficient THz-measurements with wavelengths down to  $\lambda > 100 \mu\text{m}$  (wire) or  $\lambda > 30 \mu\text{m}$  (lithographic) and no visible substructures

### 3. Improved design of a new compact and portable MPI to be operated under vacuum

The setup of the existing MPI is depicted as a drawing in Fig. 1a below. The rather bulky off-the-shelf components for large beam diameters are used inside a glass box under air or under dry nitrogen atmosphere and are mounted on a stable optical table made of steel. Since components with different coefficients of thermal expansion are mounted together tolerances and vibration control are not yet minimized. The improved design of the MPI to be operated under vacuum is depicted in Fig. 1b below. Letter Q denotes the radiation source whereas detector 1 (D1) measures a fraction of total intensity and detectors 2 and 3 (D2, D3) the autocorrelation intensity signal with orthogonal polarization state. One parabolic mirror collimates the source beam radiation to the first splitting polarizer whereas three other parabolic mirrors refocus the collimated beam onto the detectors D1 through D3. The parabolic and roof mirrors and mounts are made from one piece and have a diamond fly cutted surface with a roughness of 30 nm.

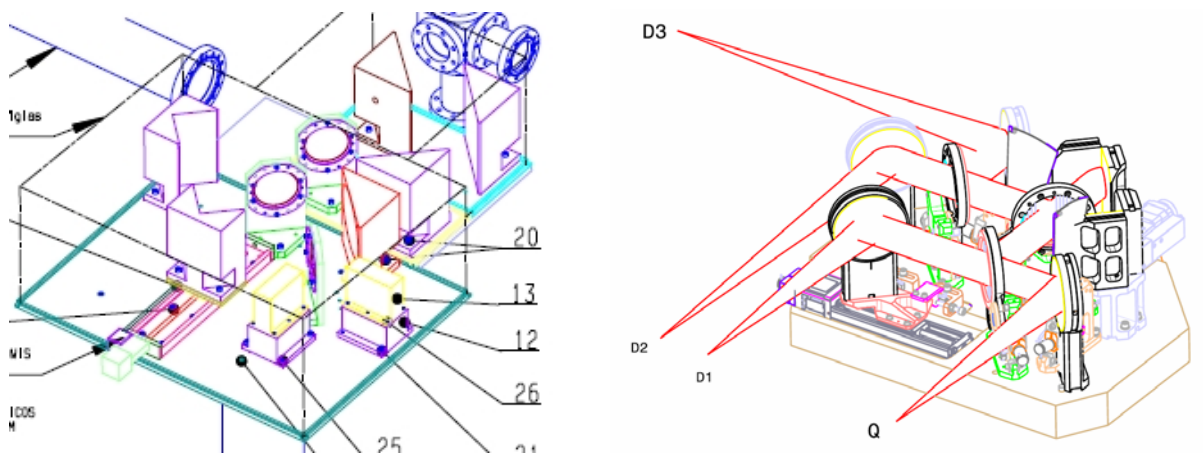


Fig 1a. Existing setup with off-the shelf components. Fig. 1b. New design with optimized components.

Apart from the polarizers and the translation stages all other components are made in-house to optimize weight, stability and precision. To reduce weight we use a high-strength aluminium alloy (AlZnMgCu1.5) for fabrication. In addition the mounts and the base plate (not shown) have a honeycomb structure. The vacuum chamber has a cover made of plastics (PMMA, for alignment purposes), thin walls and a thin bottom as well as a support with three legs and a support plate with large holes. All this contributes to minimal weight. The whole interferometer including the vacuum chamber (under 0.2 mbar) and the support has a diameter of 1m and a weight of around 100 kg.

### 4. Stability and precision

ANSYS code was used to optimize stability versus weight in the design of the vacuum chamber. The cover was segmented into symmetric slices to save computing time and to make calculations more accurate. Extra support structure on the cover results in added stiffness. Calculations for tension and deformation of the cover are visualized in the two figures below.

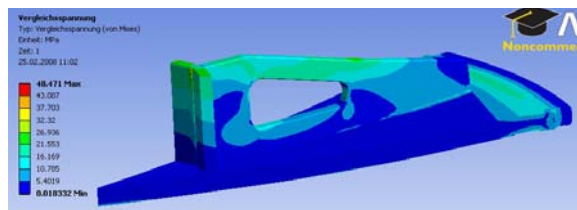


Fig 2a. Maximum stress of 33 N/mm<sup>2</sup>.

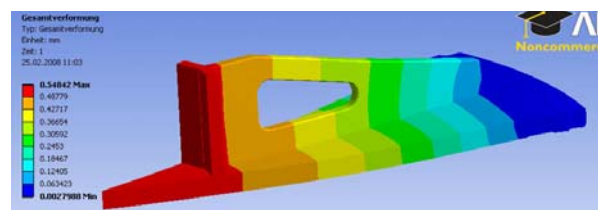


Fig. 2b. Maximum deformation of 0.55 mm.

Calculations show a maximum stress of 33 N/mm<sup>2</sup> when the cover made of PMMA is exposed to 0.2 mbar on one side and 1 bar (atmospheric pressure) on the other side. This is a factor of 1.8 below the yield strength of 70 N/mm<sup>2</sup>. Under the same pressure conditions maximum deformation in the centre is 0.55 mm with respect to the border. There is a factor of 3 above Mohr Colomb curb stress because

adjacent edges have no sharp angles and they are faceted. Since the various parts of the support structure on the cover are glued together the glue experiences tensions between  $-4$  to  $14 \text{ N/mm}^2$ .

As for the vacuum chamber made of the high-strength aluminium alloy the wall and the bottom were numerically optimized together. At the bottom a star-like reinforcement structure adds extra stability. A quarter section for the ANSYS simulation was chosen to account for the symmetry. Calculations for maximum stress and deformation are visualized in the two figures below.

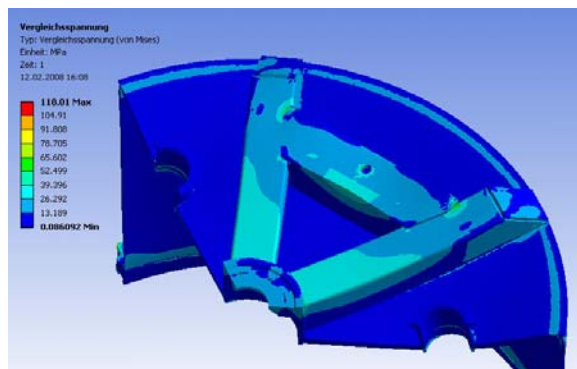


Fig 3a. Maximum stress of  $60 \text{ N/mm}^2$ .

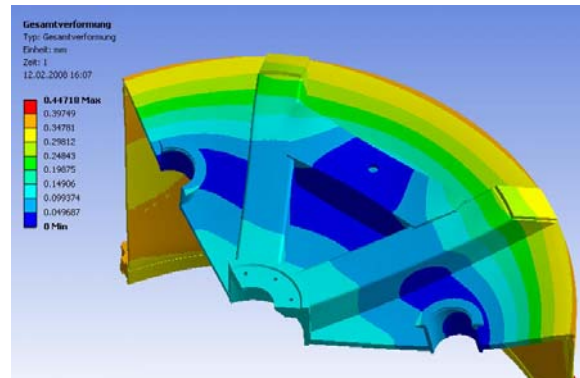


Fig. 3b. Maximum deformation of  $0.40 \text{ mm}$ .

Maximal stress of  $60 \text{ N/mm}^2$  was calculated which is a factor of 1.6 below yield strength of about  $100 \text{ N/mm}^2$  (for pure aluminium). Because of welding joints a lower yield point of a softer aluminium alloy was assumed because exact yield strength is not known for the high-tension aluminium alloy. Maximal deformation of  $0.4 \text{ mm}$  is again found in the centre with respect to the border. To summarize stress and deformations of the vacuum chamber are all within acceptable limits.

Among other details of an optimized design please note the following:

- The base plate of the support of the vacuum chamber is decoupled from the inner base plate of the interferometer. Both can be adjusted independently from each other. There is an extra transportation lock to fix the inner base plate while moving the interferometer.
- For repositioning the mounts a guiding groove and three bolts are provided. The mounts are fixed with additional two screws. Sometimes components are moved or taken out.
- The parabolic mirror which redirects a part of the incoming beam on detector 1 (sum signal) can be moved into the beam path on detector 2. This allows other detector arrangements.
- The grating polarizers can be flipped into a position where a semitransparent mirror is inserted into the beam path for alignment purposes with a visible laser.
- Beam stoppers are unfolded like a fan to block one specific beam path. Because of narrow space when not in operation they should not block unintentionally another beam path.
- Some design elements are repeated to facilitate future production of small series of interferometers. For example the fan-like beam stopper and the pair of grating polarizer and semitransparent window have the same flipping mechanism.

## 5. Conclusions and outlook

An optimized design of a Martin Puplett interferometer has been described. Compactness versus stability and precision has been demonstrated. Fabrication in our machine shop has just started. Assembly, tests and delivery are scheduled by end of August 2008.

## 6. References

- [1] Martin D.H., Infrared and Millimeter Waves 6, 65-148, chapter 2, Academic Press, 1982
- [2] Schlott V. et al., Proceedings of EPAC 2006, 1229-1231, Edinburgh, Scotland